New Method Based on Capillary Electrophoresis with Laser-Induced Fluorescence Detection (CE-LIF) to Monitor Interaction between Nanoparticles and the Amyloid-β Peptide

ARTICLE *in* ANALYTICAL CHEMISTRY · NOVEMBER 2010

Impact Factor: 5.64 · DOI: 10.1021/ac102045x · Source: PubMed

14 AUTHORS, INCLUDING:

Line De Kimpe
Becton, Dickinson and Company (BD)
19 PUBLICATIONS **489** CITATIONS
SEE PROFILE

Benjamin Le Droumaguet
Université Paris-Est Créteil Val de Marne - …
34 PUBLICATIONS **797** CITATIONS
SEE PROFILE

Mario Salmona
Mario Negri Institute for Pharmacological…
435 PUBLICATIONS **11,708** CITATIONS
SEE PROFILE

Patrick Couvreur
Université Paris-Sud 11
591 PUBLICATIONS **25,915** CITATIONS
SEE PROFILE

Anal. Chem. **2010,** *82,* 10083–10089

New Method Based on Capillary Electrophoresis with Laser-Induced Fluorescence Detection (CE-LIF) to Monitor Interaction between Nanoparticles and the Amyloid-β Peptide

Davide Brambilla,[†] Romain Verpillot,[†] Myriam Taverna,*[,†] Line De Kimpe,[‡] Benjamin Le Droumaguet,[†] Julien Nicolas,[†] Mara Canovi,[§] Marco Gobbi,[§] Francesco Mantegazza,[||] Mario Salmona,[§] Valérie Nicolas,[⊥] Wiep Scheper,[‡] Patrick Couvreur,[†] and Karine Andrieux[†]

Laboratoire de Physico-Chimie, Pharmacotechnie et Biopharmacie, UMR CNRS 8612, Univ Paris-Sud 11, Faculté de Pharmacie, 5 rue Jean-Baptiste Clément, F-92296 Chatenay-Malabry, France, Neurogenetics Laboratory, Academic Medical Center, Amsterdam, The Netherlands, Istituto di Ricerche Farmacologiche "Mario Negri", Milano, Italy, Department of Experimental Medicine, University of Milano-Bicocca, Monza, Italy, and Institut d'Innovation Thérapeutique (IFR141 ITFM), Univ Paris-Sud, Faculté de Pharmacie, 5 rue Jean-Baptiste Clément, F-92296 Châtenay-Malabry, France

A novel application of capillary electrophoresis with laser-induced fluorescence detection (CE-LIF) was proposed to efficiently detect and monitor the interaction between polymeric nanoparticles and the β-Amyloid peptide ($A\beta_{1-42}$), a biomarker for Alzheimer's Disease (AD), at concentrations close to physiological conditions. The CE-LIF method allowed the interaction between PEGylated poly(alkyl cyanoacrylate) nanoparticles (NPs) and the soluble $A\beta_{1-42}$ peptide monomers to be highlighted. These results were confirmed by surface plasmon resonance (SPR) and confocal laser scanning microscopy (CLSM). Whereas SPR showed an interaction between the NPs and the $A\beta_{1-42}$ peptide, CLSM allowed the formation of large aggregates/assemblies at high NP and peptide concentrations to be visualized. All these results suggested that these nanoparticles could bind the $A\beta_{1-42}$ peptide and influence its aggregation kinetics. Interestingly, the non-PEGylated poly(alkyl cyanoacrylate) NPs did not alter the aggregation kinetics of the $A\beta_{1-42}$ peptide, thus emphasizing the high level of discrimination of the CE-LIF method with respect to NPs.

The Alzheimer's disease (AD) is a neurodegenerative disorder characterized by a progressive loss of cognitive functions and characteristic pathological changes in the brain. It is the most common elderly dementia, affecting 35 million people worldwide.[1] It is histopathologically characterized by two main hallmarks: (i) the extracellular deposition of amyloid plaques mainly composed of β-amyloid peptides (Aβ) and (ii) intracellular neurofibrillar tangles composed of hyperphosphorylated Tau protein.[2,3] AD is a very complex disease which is likely the result of a multifactorial process strongly influenced by genetic and environmental components, but the mechanisms involved are not yet clearly understood and still under debate.[4−6]

The treatment of AD represents a crucial challenge due to incomplete understanding of the etiology and the lack of diagnostic methods able to discriminate between AD and other neurological diseases. All currently approved therapies, such as the *N*-methyl-D-aspartate (NMDA) receptor antagonist[7−9] and the acetylcholinesterase (AchE) inhibitors,[10−12] are only directed toward the alleviation of AD symptoms and exhibit many side effects.[7]

Among etiopathological hypotheses that have been proposed so far, the neuronal loss due to the toxicity of Aβ peptide aggregates, usually referred to as the "amyloid hypothesis", is one of the most widely accepted.[13,14] Aβ peptide is produced by neurons through sequential proteolytic cleavage of the amyloid precursor protein (APP) by β- and γ-secretases, forming peptides with a variable number of amino-acids, usually from 39 to 42.[15,16] Among the different species, the Aβ peptide 1−42 ($A\beta_{1-42}$) is

* To whom correspondence should be addressed. Phone: +33 (0)1 46 83 54 62. Fax: +33 (0)1 46 83 59 44. E-mail: myriam.taverna@u-psud.fr.
[†] UMR CNRS 8612, Univ. Paris Sud 11.
[‡] Academic Medical Center.
[§] Istituto di Ricerche Farmacologiche "Mario Negri".
[||] University of Milano-Bicocca.
[⊥] Institut d'Innovation Thérapeutique.

(1) Querfurth, H. W.; LaFerla, F. M. *N. Engl. J. Med.* **2010**, *362*, 329.
(2) Aguzzi, A.; O'Connor, T. *Nat. Rev. Drug Discovery* **2010**, *9*, 237.
(3) Panza, F.; Solfrizzi, V.; Frisardi, V.; Imbimbo, B. P.; Capurso, C.; D'Introno, A.; Colacicco, A. M.; Seripa, D.; Vendemiale, G.; Capurso, A.; Pilotto, A. *Aging: Clin. Exp. Res.* **2009**, *21*, 386.
(4) Aliev, G.; Smith, M. A.; de la Torre, J. C.; Perry, G. *Mitochondrion* **2004**, *4*, 649.
(5) de la Torre, J. C. *Lancet Neurol.* **2004**, *3*, 184.
(6) Korolainen, M. A.; Nyman, T. A.; Aittokallio, T.; Pirttila, T. *J. Neurochem.* **2010**, *112*, 1386.
(7) Kemp, J. A.; McKernan, R. M. *Nat. Neurosci* **2002**, *5* (Suppl), 1039.
(8) Parsons, C. G.; Danysz, W.; Quack, G. *Neuropharmacology* **1999**, *38*, 735.
(9) Reisberg, B.; Doody, R.; Stoffler, A.; Schmitt, F.; Ferris, S.; Mobius, H. J. *N. Engl. J. Med.* **2003**, *348*, 1333.
(10) Sugimoto, H.; Iimura, Y.; Yamanishi, Y.; Yamatsu, K. *J. Med. Chem.* **1995**, *38*, 4821.
(11) Munoz-Torrero, D. *Curr. Med. Chem.* **2008**, *15*, 2433.
(12) Birks, J.; Grimley Evans, J.; Iakovidou, V.; Tsolaki, M.; Holt, F. E. *Cochrane Database Syst. Rev.* **2009**, CD001191.
(13) Townsend, M.; Mehta, T.; Selkoe, D. J. *J. Biol. Chem.* **2007**, *282*, 33305.
(14) Gralle, M.; Botelho, M. G.; Wouters, F. S. *J. Biol. Chem.* **2009**, *284*, 15016.
(15) Pierrot, N.; Octave, J.-N. *Curr. Alzheimer Res.* **2008**, *5*, 92.

10.1021/ac102045x
Published on Web 11/18/2010

believed to be the most representative and the most toxic species in AD physiopathology due to its high tendency to spontaneously self-aggregate.[17,18]

The aggregation kinetics of Aβ_{1-42} peptide involves several steps and leads to the formation of species exhibiting variable sizes: typically small soluble oligomers, higher molar mass oligomers, larger protofibrils and eventually insoluble fibrils. This folding and assembly are governed by remarkably complex processes leading to multiple coexisting physical forms.

Even though it is well-known that the peptide adopts in vivo a helical conformation when it is part of the trans-membrane domain of APP,[19] spectroscopic studies have reported a random coil structure in aqueous media.[20] It may aggregate into multiple small oligomers (up to six peptides) which coalesce into intermediate assemblies.[21,22] The existence of a transitory conversion from the random coil to a helical structure upon oligomerization has been shown by nuclear magnetic resonance spectroscopy.[19] A further conformational change has been proposed, leading to soluble β-sheet aggregates and then to nonsoluble fibrils.[20]

Several therapeutic approaches targeting Aβ peptides are under investigation. Among them, one can find the design of β- and γ-secretase inhibitors[23] and monoamine oxidase inhibitors,[24−27] together with Aβ_{1-42} passive and active immunization[28,29] and dual inhibitor[30−32] strategies. More recently, the development of small molecules based on methylene blue and curcumin derivatives, which can interfere with the aggregation kinetics, may also represent a promising therapeutic approach.[33,34]

In this context, we are currently developing novel nanoparticulate systems to target and/or to influence the aggregation kinetics of the Aβ peptides. Among suitable nanocarriers, biodegradable PEGylated poly(alkyl cyanoacrylate) nanoparticles (NPs) were selected as a first candidate to investigate this new therapeutic approach due to their biodegradable properties and their well-established use for drug delivery purposes[35] as well as their in vivo ability to overpass the blood brain barrier (BBB).[36,37]

To screen the ability of our NPs to efficiently bind Aβ_{1-42}, we have for the first time applied capillary electrophoresis (CE) coupled to laser-induced fluorescence (LIF) detection to analyze fluorescently labeled Aβ. CE with UV detection has previously been used for the in vitro identification of small molecules as potential inhibitors of Aβ aggregation.[38,39] This innovative work, was however limited due to the high concentrations of peptide required for the screening, which were about 5 orders of magnitude higher than those found in vivo. More recently, Kato et al.[40] reported a CE-LIF method allowing the antiaggregation features of molecules toward fibrils to be monitored. However, those species are no longer considered to be the main toxic species for AD.[41−43] Consequently, a novel analytical method is required and must be adapted to Aβ monomers and resulting soluble oligomers.

Based on the work of De Lorenzi's research group related to the screening of antifibrillogenic activity of small molecules,[39] we report herein an analytical method able to monitor in real time the binding of soluble Aβ_{1-42} monomers to nanoparticles. Importantly, this is the first time that CE is developed to evaluate nanocarriers as potential therapeutic agents for AD treatment using in vitro conditions compatible with clinical application/trials. This analytical method was further associated to confocal laser scanning microscopy (CLSM) experiments which demonstrated a binding effect of the nanoparticles to the amyloid peptide, by influencing their aggregation kinetics. The physiological peptide concentration detectable with this method allowed nanoparticulate systems with potential binding feature to the amyloid peptide to be readily screened and quantitatively evaluated.

EXPERIMENTAL SECTION

Material and Chemicals. Poly[hexadecyl cyanoacrylate-*co*-rhodamine B cyanoacrylate-*co*-methoxypoly(ethylene glycol) cyanoacrylate] P(MePEGCA-*co*-RCA-*co*-HDCA) copolymers,[44] poly-[hexadecyl cyanoacrylate-*co*-methoxypoly(ethylene glycol) cyano-

(16) Chow, V. W.; Mattson, M. P.; Wong, P. C.; Gleichmann, M. *NeuroMol. Med.* **2009**, *12*, 1.
(17) Garcia-Matas, S.; de Vera, N.; Aznar, A. O.; Marimon, J. M.; Adell, A.; Planas, A. M.; Cristofol, R.; Sanfeliu, C. *J. Alzheimer's Dis.* **2010**, *20*, 229.
(18) Allaman, I.; Gavillet, M.; Belanger, M.; Laroche, T.; Viertl, D.; Lashuel, H. A.; Magistretti, P. J. *J. Neurosci.* **2010**, *30*, 3326.
(19) Crescenzi, O.; Tomaselli, S.; Guerrini, R.; Salvadori, S.; D'Ursi, A. M.; Temussi, P. A.; Picone, D. *Eur. J. Biochem.* **2002**, *269*, 5642.
(20) Tomaselli, S.; Esposito, V.; Vangone, P.; van Nuland, N. A.; Bonvin, A. M.; Guerrini, R.; Tancredi, T.; Temussi, P. A.; Picone, D. *ChemBioChem* **2006**, *7*, 257.
(21) Kayed, R.; Head, E.; Thompson, J. L.; McIntire, T. M.; Milton, S. C.; Cotman, C. W.; Glabe, C. G. *Science* **2003**, *300*, 486.
(22) Klein, W. L.; Krafft, G. A.; Finch, C. E. *Trends Neurosci.* **2001**, *24*, 219.
(23) Shao, D.; Zou, C.; Luo, C.; Tang, X.; Li, Y. *Bioorg. Med. Chem. Lett.* **2004**, *14*, 4639.
(24) Sano, M.; Ernesto, C.; Thomas, R. G.; Klauber, M. R.; Schafer, K.; Grundman, M.; Woodbury, P.; Growdon, J.; Cotman, C. W.; Pfeiffer, E.; Schneider, L. S.; Thal, L. J. *N. Engl. J. Med.* **1997**, *336*, 1216.
(25) Riederer, P.; Danielczyk, W.; Grunblatt, E. *Neurotoxicology* **2004**, *25*, 271.
(26) Youdim, M. B. H.; Buccafusco, J. J. *Trends Pharmacol. Sci.* **2005**, *26*, 27.
(27) Huang, W.; Chen, Y.; Shohami, E.; Weinstock, M. *Eur. J. Pharmacol.* **1999**, *366*, 127.
(28) Zou, J.; Yao, Z.; Zhang, G.; Wang, H.; Xu, J.; Yew, D. T.; Forster, E. L. *J. Neurol. Sci.* **2008**, *272*, 87.
(29) Dodart, J. C.; Bales, K. R.; Paul, S. M. *Trends Mol. Med.* **2003**, *9*, 85.
(30) Bolognesi, M. L.; Andrisano, V.; Bartolini, M.; Banzi, R.; Melchiorre, C. *J. Med. Chem.* **2005**, *48*, 24.
(31) Camps, P.; Formosa, X.; Munoz-Torrero, D.; Petrignet, J.; Badia, A.; Clos, M. V. *J. Med. Chem.* **2005**, *48*, 1701.
(32) Toda, N.; Tago, K.; Marumoto, S.; Takami, K.; Ori, M.; Yamada, N.; Koyama, K.; Naruto, S.; Abe, K.; Yamazaki, R.; Hara, T.; Aoyagi, A.; Abe, Y.; Kaneko, T.; Kogen, H. *Bioorg. Med. Chem.* **2003**, *11*, 1935.
(33) Yadav, A.; Sonker, M. *Eur. J. Med. Chem.* **2009**, *44*, 3866.
(34) Hawkes, C. A.; Deng, L. H.; Shaw, J. E.; Nitz, M.; McLaurin, J. *Eur. J. Neurosci.* **2010**, *31*, 203.
(35) Nicolas, J.; Couvreur, P. *Wiley Interdiscip. Rev.: Nanomed. Nanobiotechnol.* **2009**, *1*, 111.
(36) Andrieux, K.; Couvreur, P. *Wiley Interdiscip. Rev.: Nanomed. Nanobiotechnol.* **2009**, *1*, 463.
(37) Brigger, I.; Morizet, J.; Aubert, G.; Chacun, H.; Terrier-Lacombe, M. J.; Couvreur, P.; Vassal, G. *J. Pharmacol. Exp. Ther.* **2002**, *303*, 928.
(38) Sabella, S.; Quaglia, M.; Lanni, C.; Racchi, M.; Govoni, S.; Caccialanza, G.; Calligaro, A.; Bellotti, V.; De Lorenzi, E. *Electrophoresis* **2004**, *25*, 3186.
(39) Colombo, R.; Carotti, A.; Catto, M.; Racchi, M.; Lanni, C.; Verga, L.; Caccialanza, G.; De Lorenzi, E. *Electrophoresis* **2009**, *30*, 1418.
(40) Kato, M.; Kinoshita, H.; Enokita, M.; Hori, Y.; Hashimoto, T.; Iwatsubo, T.; Toyo'oka, T. *Anal. Chem.* **2007**, *79*, 4887.
(41) Dahlgren, K. N.; Manelli, A. M.; Stine, W. B., Jr.; Baker, L. K.; Krafft, G. A.; LaDu, M. J. *J. Biol. Chem.* **2002**, *277*, 32046.
(42) Cizas, P.; Budvytyte, R.; Morkuniene, R.; Moldovan, R.; Broccio, M.; Losche, M.; Niaura, G.; Valincius, G.; Borutaite, V. *Arch. Biochem. Biophys.* **2010**, *496*, 84.
(43) Roychaudhuri, R.; Yang, M.; Hoshi, M. M.; Teplow, D. B. *J. Biol. Chem.* **2009**, *284*, 4749.
(44) Brambilla, D.; Nicolas, J.; Droumaguet, B. L.; Andrieux, K.; Marsaud, V.; Couraud, P.-O.; Couvreur, P. *Chem. Commun. (Cambridge, U. K.)* **2010**, *46*, 2602.

acrylate] P(MePEGCA-*co*-HDCA) copolymers[35] and poly(hexadecyl cyanoacrylate) PHDCA homopolymers[37] were obtained following previously reported procedures. NaH_2PO_4 (>99%) was purchased from Merck & Co (Fontenay Sous Bois, France), Na_2HPO_4 (>98%) was obtained from Prolabo (Strasbourg, France), thioflavin (99%), ammonium hydroxide (NH_4OH) 28.1% (m/V), Pluronic F-68 (99%), 1,1,1,3,3,3-hexafluoro-2-propanol (HFIP) (99.8%), dimethyl sulfoxide (99.5%), sodium dodecyl sulfate (SDS, 99%), acetic acid (99%), sodium acetate (99%), bovine serum albumin (BSA, 99%) and ethanolamine (99%) were purchased from Sigma-Aldrich (St. Quentin Fallavier, France). Sodium hydroxide (NaOH, 1 M) was obtained from VWR (Fontenay-sous Bois, France). Acetone was purchased at the highest grade from Carlo Erba (Val de Reuil, France). Lyophilized HiLyte Fluor 488 labeled Aβ_{1-42} and Aβ_{1-42} peptides were provided by ANASPEC (Le Perray en Yvelines, France). Anti-Aβ antibody 6E10 was from Covance (Princeton, New Jersey).

APPARATUS

Capillary Electrophoresis. CE was performed on PA 800 instrument (Beckman Coulter, Roissy, France) using uncoated silica capillaries (Phymep, Paris) with an internal diameter of 50 μm and 50 cm total length (40 cm effective length was employed for the separation). All buffers were prepared with deionized water and were filtered through a 0.22 μm membrane (VWR) before use. Before analysis, the capillaries were preconditioned by the following rinsing sequence: 0.1 M NaOH for 5 min, 1 M NaOH for 5 min and then deionized water for 5 min. The in-between-runs rinsing cycles were carried out by pumping sequentially through the capillary: water for 5 min, 50 mM SDS for 2 min (to inhibit the aggregation and subsequent peptide adsorption on the capillary wall),[45] and 0.1 M NaOH for 5 min. The samples were introduced into the capillary by hydrodynamic injection under 3.4 kPa. The capillary was thermostated at 25 °C and the samples were maintained at 37 °C by the storage sample module of the PA 800 apparatus. The separations were carried out at 16 kV with positive polarity at the inlet using 80 mM phosphate buffer pH 7.4. The electrolyte was renewed after each run. The peptides were detected by a laser-induced fluorescence (LIF) detection system equipped with 3.5 mW argon-ion laser with a wavelength excitation of 488 nm, the emission being collected through a 520 nm band-pass filter or by diode-array detector (DAD) at 190 nm. Peak areas were estimated using the 32 Karat software (Beckman Coulter).

Confocal Laser Scanning Microscope. Observations were made by sequential acquisition with a Zeiss LSM-510 confocal scanning laser microscope equipped with a 30 mW argon laser and 1 mW helium neon laser, using a Plan-Apochromat 63X objective lens (NA 1.40, oil immersion). Red fluorescence was observed with a long-pass 560 nm emission filter and under a 543 nm laser illumination. Green fluorescence was observed with a band-pass 505 and 550 nm emission filter and under a 488 nm laser illumination. The pinhole diameter was set at 61 μm giving an optical section thickness of 0.6 μm. Stacks of images were collected every 0.3 μm along the *z* axis. Twelve bit numerical images were acquired with LSM 510 software version 3.2.

SPR Apparatus. ProteOn XPR36 (Biorad) apparatus, which has six parallel flow channels that can be used to uniformly immobilize strips of six ligands on the sensor surface, was employed. The fluidic system of Proteon XPR36 can automatically rotate 90° so that up to six different analytes (e.g., different nanoparticle preparations, or different concentrations of the same nanoparticle) can be injected simultaneously over all the different immobilized molecules. All the injections were carried out for 3 min at a flow rate of 30 μL·min^{-1} at 30 °C in PBST (phosphate buffer saline +0.005% Tween20, pH 7.4).

METHODS

Nanoparticle Preparation. Fluorescent and nonfluorescent nanoparticles were prepared using P(MePEGCA-*co*-RCA-*co*-HDCA), P(MePEGCA-*co*-HDCA) copolymers, and PHDCA homopolymer according to protocols recently published by our group.[44] The (co)polymer (10 mg) was dissolved in acetone (2 mL) and this solution was added dropwise to an aqueous solution 0.5% (w/v) of Pluronic F-68 (4 mL) under vigorous mechanical stirring. A milky suspension was observed almost instantaneously. Acetone was then evaporated under reduced pressure and nanoparticles were purified by ultracentrifugation (150 000*g*, 1 h, 4 °C, Beckman Coulter, Inc.). The supernatant was discarded and the pellet was resuspended in the appropriate volume of deionized water to yield a 2.5 mg·mL^{-1} nanoparticle suspension.

Nanoparticle Characterization. The nanoparticle diameter (D_z) was measured by dynamic light scattering (DLS) with a Nano ZS from Malvern (173° scattering angle) at 25 °C. DLS measurements were used to monitor the nanoparticles stability as a function of time upon their incubation at 37 °C in the buffer employed for capillary electrophoresis experiments. The nanoparticle surface charge was investigated by ζ-potential measurement at 25 °C after dilution with 1 mM NaCl solution applying the Smoluchowski equation and using the same apparatus.

Peptide Sample Preparation and Storage. Lyophilized Aβ_{1-42} and HiLyte Fluor labeled Aβ_{1-42} peptide were dissolved in 0.16% (m/V) ammonium hydroxide aqueous solution to reach a concentration of 2 mg·mL^{-1}. The fluorescent and nonlabeled peptide solutions were then divided into aliquots individually stored at −20 °C which were freshly defrosted prior analysis.

The Aβ_{1-42} peptide used for SPR experiments was prepared from a depsi-Aβ_{1-42} peptide synthesized as previously described.[46] This depsi-peptide is much more soluble than the native peptide and has also a much lower propensity to aggregate, thus preventing the spontaneous formation of "seeds" in solution.[46] The native Aβ_{1-42} peptide was then obtained from the depsi-peptide by a "switching" procedure involving a change in pH.[46,47] The Aβ_{1-42} peptide solution obtained immediately after switching was shown to be free of seed. The Aβ_{1-42} peptide obtained by this procedure is

(45) Han, Y.; He, C.; Cao, M.; Huang, X.; Wang, Y.; Li, Z. *Langmuir* **2009**, *26*, 1583.
(46) Taniguchi, A.; Sohma, Y.; Hirayama, Y.; Mukai, H.; Kimura, T.; Hayashi, Y.; Matsuzaki, K.; Kiso, Y. *ChemBioChem* **2009**, *10*, 710.
(47) Balducci, C.; Beeg, M.; Stravalaci, M.; Bastone, A.; Sclip, A.; Biasini, E.; Tapella, L.; Colombo, L.; Manzoni, C.; Borsello, T.; Chiesa, R.; Gobbi, M.; Salmona, M.; Forloni, G. *Proc. Natl. Acad. Sci. U.S.A.* **2010**, *107*, 2295.
(48) Atha, D. H.; Ingham, K. C. *J. Biol. Chem.* **1981**, *256*, 12108.
(49) Shulgin, I. L.; Ruckenstein, E. *Biophys. Chem.* **2006**, *120*, 188.
(50) Auer, S.; Trovato, A.; Vendruscolo, M. *PLoS Comput. Biol.* **2009**, *5*, e1000458.
(51) Chiti, F.; Dobson, C. M. *Annu. Rev. Biochem.* **2006**, *75*, 333.

therefore in its original state and, for the sake of simplicity; it will be referred here to as the "monomer". Further characterizations, carried out by Gobbi's group, indicated that the Aβ "monomer" used for the present study gave no thioflavin T (ThT) signal and was unstructured as observed by circular dichroism (manuscript submitted, 2010).

The peptide concentration required for the different methods described below were not strictly the same as long as different detection thresholds had to be taken into account.

Capillary Electrophoresis Experiments. To study the interaction between the monomeric form of the Aβ_{1-42} peptide and the nanoparticles, aliquots of HiLyte Fluor labeled Aβ_{1-42} peptide stock solutions were diluted in 20 mM phosphate buffer (NaH_2PO_4) at pH 7.4 containing a 20 μM P(MePEGCA-*co*-RCA-*co*-HDCA) nanoparticle suspension to obtain final peptide concentrations of 5, 1, 0.5, and 0.05 μM. The samples were then incubated at 37 °C and analyzed by capillary electrophoresis every 2 h. The same protocol was followed with P(MePEGCA-*co*-RCA-*co*-HDCA) nanoparticle suspension or Aβ_{1-42} peptide solution.

Similarly, a mixture of nonfluorescent P(MePEGCA-*co*-HDCA) or PHDCA nanoparticle suspensions (20 μM final concentration) and Aβ_{1-42} at 10 μM were analyzed by CE using the DAD detector at 190 nm as control.

These experiments allowed the evolution of % monomer peak as a function of incubation time to be determined. % monomer peak is calculated as the ratio between the absolute peak area of the monomer observed at $t = 0$ and the one observed at each incubation time.

Surface Plasmon Resonance Experiments. Aβ_{1-42} monomers were immobilized in parallel-flow channels of a GLC sensor chip (Biorad) using amine-coupling chemistry. Briefly, after surface activation the peptide solutions (10 μM in acetate buffer pH 4.0) were injected for 5 min at a flow rate of 30 $\mu L \cdot min^{-1}$ and the remaining activated groups were blocked with ethanolamine at pH 8.0. The final immobilization levels were about 2500 resonance units (1 RU = 1 pg protein$\cdot mm^{-2}$). Bovine serum albumin (BSA) was immobilized, in a parallel flow channel as a reference protein. Another reference surface was prepared in parallel using the same immobilization procedure but without addition of the peptide (naked surface). Before performing experiments with nanoparticles, we checked that Aβ species immobilized can bind with high affinity to the anti-Aβ antibody 6E10 (see Supporting Information (SI) Figure S6c). The suspension of P(MePEGCA-*co*-HDCA) NPs was diluted at different concentrations (0.3−20 μM) and flowed into the machine simultaneously.

Confocal Laser Scanning Microscopy Analysis. The interaction between the polymeric nanoparticles and the Aβ_{1-42} peptide was investigated by confocal laser scanning microscopy (CLSM) using HiLyte Fluor labeled Aβ_{1-42} peptide and rhodamine B-labeled P(MePEGCA-*co*-RCA-*co*-HDCA) NPs.

The Aβ_{1-42} peptide aliquots were defrosted, immediately diluted with 20 mM phosphate buffer and incubated with 20 μM nanoparticle suspension to reach a final peptide concentration of 10, 1, or 0.05 μM. A 10 μL deposit of this final incubation sample on glass coverslips was immediately analyzed by CLSM. The remaining suspensions were incubated at 37 °C and, after 12 h, another 10 μL was withdrawn from the suspension and analyzed in the same manner by CLSM.

Thioflavin T Aggregation Assay. Aβ_{1-42} was dissolved in hexafluoroisopropanol (HFIP) at a final concentration of 1 $mg \cdot mL^{-1}$, sampled and allowed to evaporate. For coaggregation experiments, the peptide film was first dissolved in DMSO and sonicated in a bath sonicator for 10 min. Subsequently, Aβ_{1-42} was diluted in phosphate-buffer saline (PBS, 20 mM sodium phosphate buffer, pH 7.4, containing 137 mM NaCl) to a final concentration of 50 μM. This mixture was aggregated in the presence or absence of P(MePEGCA-*co*-RCA-*co*-HDCA) NPs for 24 h at 37 °C. Aggregated Aβ_{1-42} was diluted to a final concentration of 5 μM into 50 mM glycine buffer at pH 7.4 containing 10 μM ThT. Fluorescence was measured in 96 well nonbinding plates (Greiner Bio One, Frickenhausen, Germany) using a Fluostar Omega microplate reader at an excitation wavelength of 450 nm and emission at 485 nm.

RESULTS AND DISCUSSION

The purified fluorescent and nonfluorescent nanoparticles prepared by nanoprecipitation were characterized by DLS and ζ-potential measurements. PEGylated nanoparticles presented an average diameter in the 90−100 nm range with narrow particle size distribution, whereas non-PEGylated counterparts were centered around 160 nm (see SI Figure S1). Those nanoparticles exhibited a negative ζ-potential (−30 ± 5 mV), which is in a suitable window for biomedical applications. Notably all kinds of nanoparticles showed good colloidal stability in the capillary electrophoresis buffer (i.e., phosphate buffer pH 7.4, 20 mM) as assessed by DLS measurement during 72 h (SI Figure S1).

The CE-LIF method described in this study was developed to investigate the interaction between rhodamine B-labeled nanoparticles and HiLyte Fluor labeled Aβ_{1-42}. The LIF detection allowed a lower concentration of peptide to be used than with UV detection, in order to better fit with physiological processes and conditions. Indeed, Aβ peptide is found in biological fluids, such as the cerebro-spinal fluid (CSF), at nanomolar concentrations and therefore a sensitive and discriminative analytical method is required.

The CE-LIF analysis of a solution of the fluorescent Aβ_{1-42} showed a single peak migrating at ~7.5 min (with a highly reproducible migration time for each batch) and mainly constituted by the monomeric form. Interestingly, the electrophoretic profile of the peptide sample stayed constant over time up to 24 h (Figure 1a), thus demonstrating an excellent stability of the fluorescent peptide in its monomeric form at this concentration in the buffer.

Remarkably, when the same concentration of Aβ_{1-42} peptide solution was incubated with 20 μM of fluorescent P(MePEGCA-*co*-RCA-*co*-HDCA) nanoparticle suspension, a gradual decrease of the monomeric peptide peak was observed (Figure 1b). These results indicate an interaction between the peptide and the nanoparticles. In order to validate this finding, the method was then applied to other NPs with different surface features; namely non-PEGylated poly(hexadecyl cyanoacrylate) (PHDCA) nanoparticles. Interestingly, no variation of the monomer peak was

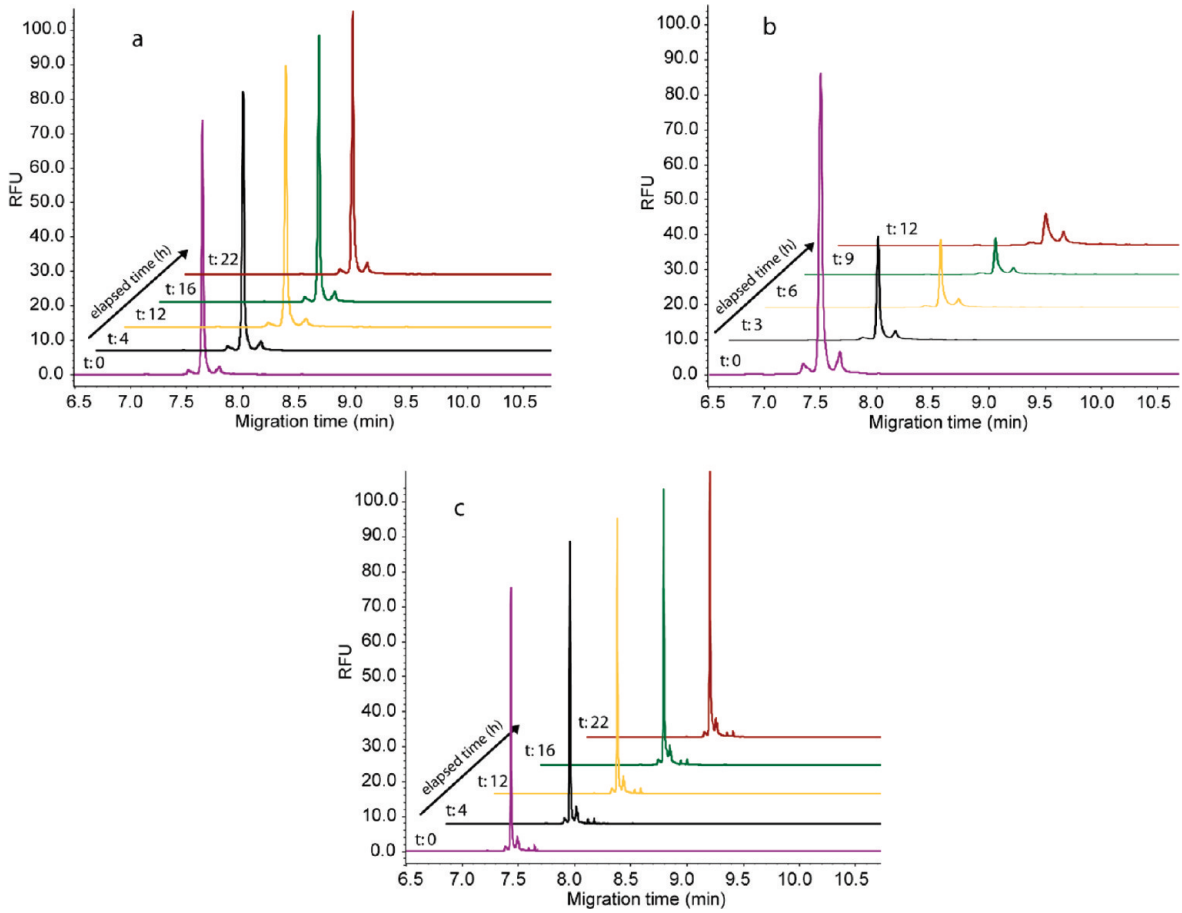

Figure 1. (a) Evolution of the CE-LIF profile as a function of time at 37 °C of a 5 μM Hilyte Fluor Aβ_{1-42} solution alone and (b) in the presence of a 20 μM P(MePEGCA-*co*-RCA-*co*-HDCA) nanoparticle suspension and (c) in the presence of a 20 μM PHDCA nanoparticle suspension.

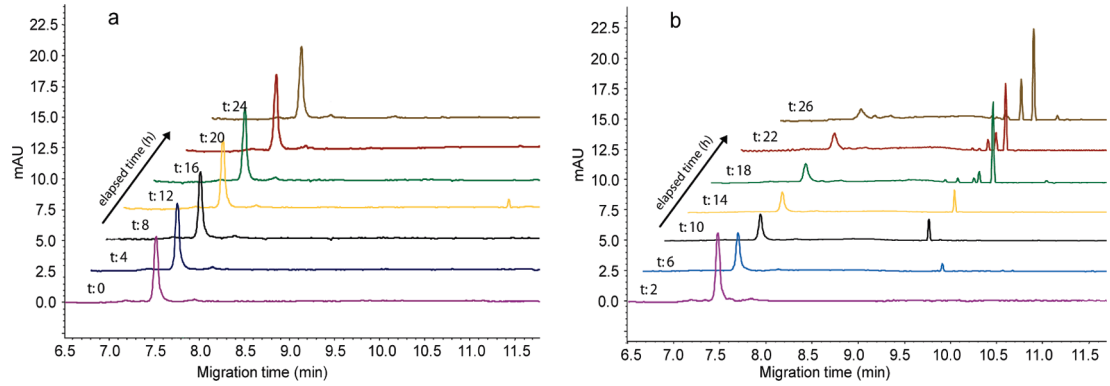

Figure 2. Evolution of the CE-UV profile as a function of time at 37 °C of (a) a 10 μM Aβ_{1-42} solution alone and (b) a 10 μM Aβ_{1-42} solution incubated with a 20 μM P(MePEGCA-*co*-HDCA) nanoparticle suspension.

observed over time upon incubation with PHDCA NPs under the same experimental conditions as the PEGylated counterparts (Figure 1c). It is well-known that PEG chains can interplay with protein environment altering their solubility in aqueous media,[48] although the mechanism has not yet been fully elucidated.[49] In our case, it is believed that PEG chains locally modified the peptide solubility and thus triggered its uptake by the nanoparticles. Therefore, these results confirm that the analytical method presented in this study is able to efficiently discriminate nanoparticles with respect to their respective aptitude to bind Aβ_{1-42}.

Similar experiments were then performed with nonfluorescent peptide and NPs to confirm the previous findings and check whether the fluorescent tags could have altered the binding behavior observed so far. To this purpose, CE with UV detection was employed for the monitoring and similar results were obtained than with fluorescent Aβ_{1-42} and rhodamine B-tagged NPs (Figure 2). In addition, multiple spikes exhibiting migration times around 10−11 min appeared after a 6 h incubation time period on the corresponding profile (Figure 2b). These peaks, the intensity and number of which increased as a function of time, were assigned to the association between nonlabeled peptide

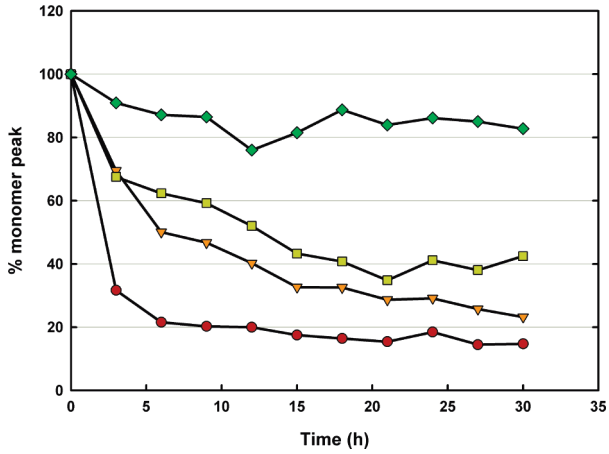

Figure 3. Aβ_{1-42} monomer peak intensity as a function of time upon incubation of Aβ_{1-42} in the presence of fluorescent P(MePEGCA-*co*-HDCA) NPs at 20 μM. The concentration of Aβ_{1-42} was 0.05 μM (◆), 0.5 μM (■), 1 μM (▼), or 5 μM (●).

species and the nanoparticles. However, these peaks were not observed with the CE-LIF method likely due to optical features of the LIF detection.

The CE-LIF method was also used to evaluate the kinetics of disappearance of the monomeric peptide as a function of the concentration ratio between P(MePEGCA-*co*-RCA-*co*-HDCA) NPs and Aβ_{1-42}. As shown in Figure 3, whatever the concentration ratio, there was a clear uptake of peptide by the NPs (capture varying from 20 to 85%) but this process was strictly dependent on the peptide availability in solution. The higher the initial peptide concentration, the faster and the higher the capture. Assuming in a first approach that the Aβ_{1-42}-NPs interaction was governed by a first-order kinetic, we have estimated the affinity constant, k_d, for this interaction to be 0.55 μM (see SI Figures S2 and S3). Interestingly, for the highest peptide concentrations, we observed a nonlinear disappearance of the monomeric peak over time suggesting the formation of peptide aggregates at the surface of the nanoparticles. Interestingly in the absence of nanoparticles, the peptide did not spontaneously form any aggregate in the concentration range (0.05−5 μM) of this experiment.

To investigate whether the P(MePEGCA-*co*-HDCA) NPs could indeed influence the aggregation kinetics of Aβ_{1-42}, we performed a Thioflavin T assay in the absence or in the presence of these NPs. ThT experiments performed at high peptide concentration (50 μM), favoring its aggregation, confirmed that the P(MePEGCA-*co*-HDCA) NPs strongly increased Aβ_{1-42} aggregation (SI Figure S4). Therefore, it is reasonable to assume that the aggregation of peptides was initiated by nanoparticle surfaces. This hypothesis is fully supported by previous computational work reported by Auer et al.[50] about the catalyzed/acceleration of peptide aggregation by nanoparticles.

CLSM was then employed for two main reasons: (i) to have a direct visualization of the binding process and thus to confirm previous results obtained by CE-LIF and (ii) to have a better insight into the nature of the aggregates that formed at the surface of the NPs. The P(MePEGCA-*co*-RCA-*co*-HDCA) nanoparticle

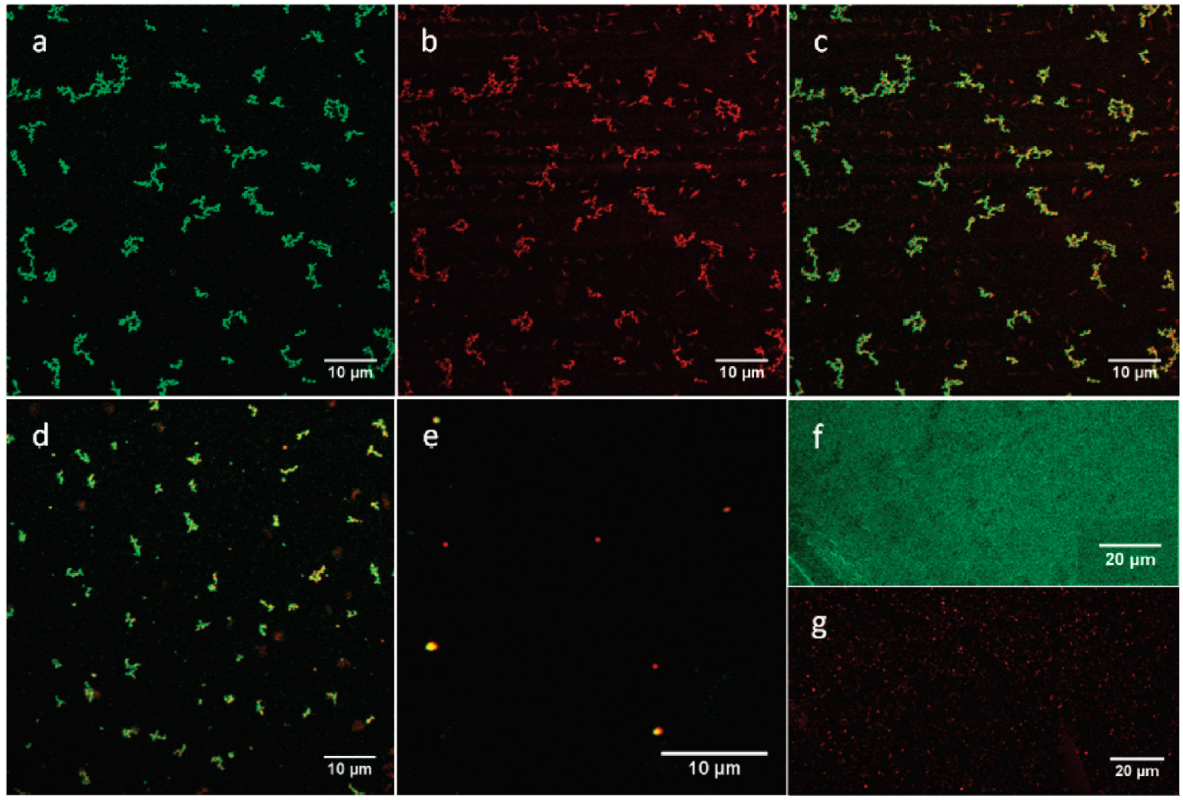

Figure 4. Confocal microscopy images showing colocalization of Hilyte Fluor Aβ_{1-42} and P(MePEGCA-*co*-RCA-*co*-HDCA) nanoparticle suspension after their incubation for 12 h. (a) Aβ_{1-42} peptide (10 μM) (green channel) (b) P(MePEGCA-*co*-RCA-*co*-HDCA) nanoparticles (20 μM) (red channel) (c) merge of (a) and (b). Effect of the peptide concentration on the size of the assemblies: (d) solution of Hilyte Fluor Aβ_{1-42} (1 μM) and P(MePEGCA-*co*-RCA-*co*-HDCA) nanoparticles (20 μM); (e) solution of Hilyte Fluor Aβ_{1-42} (50 nM) and P(MePEGCA-*co*-RCA-*co*-HDCA) nanoparticles (20 μM). Control experiments: (f) solution of Hilyte Fluor Aβ_{1-42} (10 μM) and (g) P(MePEGCA-*co*-RCA-*co*-HDCA) nanoparticles (20 μM).

suspension was added to fluorescent $A\beta_{1-42}$ solution at different ratios ($[A\beta]_0 = 0.05-10\ \mu M$) and the resulting samples were observed immediately after mixing (time zero) and after a 12 h incubation time period at 37 °C. At time zero, a faint colocalization was observed (SI Figure S5). After 12 h of incubation, a complete colocalization of green (fluorescent peptide) and red (rhodamine B-labeled nanoparticles) channels was observed (Figure 4) evidencing a strong NP-peptide interaction. Moreover, a proportional decrease of the size of these dual-fluorescent assemblies was noticed as a function of the $[A\beta]_0/[NPs]_0$ ratio (Figure 4). For the lowest peptide concentration, no aggregate was formed (Figure 4e) suggesting that the aggregation threshold was not reached.

According to the literature, peptide aggregation is concentration-dependent and the nucleation reaction is believed to be the rate limiting step.[51] It can be therefore hypothesized that, when there is an affinity between the peptide and some nanoparticles, the interaction of the peptide with the nanoparticle surface increases its local concentration, reaching the nucleation threshold which then triggers the aggregation process.

At the highest concentrations, the formation of aggregates and their size modulation could be explained by a self-aggregation of the PEGylated nanoparticles driven by the presence of monomeric and/or peptide oligomers on their surface and this was thereby directly proportional to the amount of peptide available in solution. These microscopy observations fully support the CE results regarding the ability of PEGylated poly(alkyl cyanoacrylate) nanoparticles to bind the $A\beta_{1-42}$ monomer and to promote its aggregation at their surface, leading to large aggregate formation only at the highest concentrations of peptides. Moreover, due to the size of those assemblies, it is possible to envision that once the nucleation process is triggered at the nanoparticle surface, the aggregation takes place, creating also oligomer bridges between NPs.

To our knowledge, this is the first time that interaction between polymeric nanoparticles and $A\beta_{1-42}$ peptide in solution is experimentally monitored, described and quantified. Finally, the nanoparticle ability to interact with the $A\beta_{1-42}$ peptide, highlighted by CE and confocal microscopy was evaluated by SPR experiments used as a complementary method. Increasing concentrations (0.3, 3, and 20 μM) of a suspension of P(MePEGCA-*co*-RCA-*co*-HDCA) NPs were flowed over a chip coated with the monomeric $A\beta_{1-42}$ for 3 min. The resulting sensorgrams clearly showed a concentration-dependent interaction between the PEGylated nanoparticles and the peptide immobilized onto the chip (SI Figure S6a). As a control, the same experiment was performed on a BSA-coated chip and revealed no interaction with the nanoparticles (SI Figure S6b). This is quite striking as long as BSA is usually considered as a "sticky" protein that binds many other proteins, surfaces and molecules. These SPR results confirmed the interaction between PEGylated NPs and the $A\beta_{1-42}$ peptide.

CONCLUSIONS

In this work for the first time a method relying on CE-LIF was proposed to evidence the ability of polymeric nanoparticles to bind the $A\beta_{1-42}$ peptide, the main molecular species involved in the pathological process of neurodegeneration in AD.

To this end, we have highlighted an interaction between PEGylated poly(alkyl cyanoacrylate) nanoparticles and $A\beta_{1-42}$. Importantly, combining these results with confocal microscopy and surface plasmon resonance demonstrates that these nanoparticles can bind $A\beta_{1-42}$ and influence its aggregation kinetics. Further experiments are under progress in order to elucidate the role of PEG chains in the binding mechanism with $A\beta_{1-42}$. However, the difference observed between PEGylated and non-PEGylated nanoparticles underlined the utility of the CE-LIF technique.

The proposed method exhibits high sensitivity, rapid analysis, and great ability to mimic in vivo conditions. In contrast, other techniques such as SPR and Thioflavin T assay required immobilized or higher concentrations of peptide, respectively, which do not match with physiological conditions. Therefore, CE-LIF represents a clear advance and could open new routes for the screening of novel nanoparticle-based drugs for amyloidogenic pathology treatment but also for the detection of $A\beta$ amyloid peptide from CSF to propose an early diagnosis of AD.

ACKNOWLEDGMENT

The research leading to these results has received funding from the European Community's Seventh Framework Programme (FP7/2007−2013) under agreement n°212043. The CNRS and the French Ministry of Research are also warmly acknowledged for financial support. D.B. and R.V. contributed equally to this work.

SUPPORTING INFORMATION AVAILABLE

Figure S1: Stability of nanoparticles; Figure S2: Curve fitting to experimental plots from Figure 3; Figure S3: k_{obs} vs peptide concentration plots; Figure S4: ThT assay experiment results; Figure S5: CLSM images at time = 0 of P(MePEGCA-*co*-RCA-*co*-HDCA) nanoparticles and Hilyte $A\beta_{1-42}$ peptide; Figure S6: SPR sensograms. This material is available free of charge via the Internet at http://pubs.acs.org.

Received for review August 2, 2010. Accepted November 3, 2010.

AC102045X